Neuromuscular

had no *PMP22* rearrangement or patients with the axonal type of CMT, genomic DNA was extracted from their peripheral blood leucocytes, and then 30 disease-causing genes related to CMT were screened for using the custom MyGeneChip CustomSeq Resequencing Array (Affymetrix, Inc, Santa Clara, California, USA), which was designed to screen for CMT and related diseases, such as ataxia with oculomotor apraxia types 1 and 2, spinocerebellar ataxia with axonal neuropathy and distal hereditary motor neuropathy.[10] We designed 363 primer sets to include the entire coding regions and flanking sequences of the 30 genes (box 1). When a novel mutation was detected, we performed familial segregation analysis to elucidate the pathogenicity of the mutation if possible.

Ultrasound

All US examinations were performed by the same examiner (Y-iN) trained in neuromuscular US, using a GE Logic P5 System (GE Healthcare Japan, Tokyo, Japan) with a 12 MHz linear-array probe. The cross-sectional areas (CSAs) of the following nerves and nerve roots were measured: median nerve, sural nerve, great auricular nerves and C6 nerve root. Additionally, the diameter of the C6 root was measured. The median and the sural nerves were selected for evaluation because those nerves have been frequently evaluated in preceding studies in patients with CMT. The greater auricular nerve was examined because of the unique travelling course in the neck surface and its easy accessibility. The examiner (Y-iN) was not blinded to the diagnosis or clinical or electrophysiological findings. All participants were placed in a supine position when

their median nerves and cervical nerve roots were examined, and in a prone position when their sural nerves were examined. The median nerve was imaged at the wrist crease, in the middle of the forearm, and in the middle of the upper arm. The sural nerve was imaged at 10 cm proximal to the lateral malleolus. We used the saphenous vein as a landmark when we identified the sural nerve beside the vein. The great auricular nerve was imaged at the midpoint between the top of the sternum and mandibular angle. We could identify the nerve in front of the sternocleidomastoid muscle (figure 1A). The CSAs were calculated by manual tracking of the nerve circumference including the hyperechoic rim. The diameter of the root was measured between the outer surfaces of the hyperechoic rims. The measured site of the C6 nerve root was about 1 cm distal to the transverse process after identifying the C6 vertebra using a previously reported procedure (figure 1B).[11]

Nerve conduction studies

Using standard techniques (Neuropack EMG system (Nihon Kohden, Tokyo, Japan)), conventional NCS was performed. The skin temperature was maintained above 32°C. The distal motor latency (DML), compound muscle action potential (CMAP) amplitude and MCV were recorded from the median nerve. The MCV was assessed in the wrist to elbow. The sensory nerve action potential (SNAP) amplitude, SNAP duration and sensory conduction velocity (SCV) were recorded from median and sural nerves. Antidromic median and sural nerve SNAPs were recorded from digit II and behind the lateral malleolus, respectively. We analysed the corresponding nerves in unilateral side using US and NCS.

Clinical assessment

Patients with CMT underwent clinical and neurophysiological assessment based on the CMT Neuropathy Score (CMTNS).[12] The CMTNS is composed of nine items: sensory symptoms, motor symptoms of legs and arms, pin sensibility, vibration, strength of legs and arms, ulnar CMAP amplitude and ulnar SNAP amplitude. The CMTNS ranges from 0 (no deficit) to 36 (maximal deficit).

Statistics

In the analysis of NCS parameters, if no CMAP and SNAP responses were elicited, they were excluded from analysis except for the amplitude data (CMAP and SNAP amplitudes in no response were regarded as 0.001 mV and 0.001 μV, respectively). Fisher's exact test was used to analyse the gender ratio between patients with CMT and controls. To compare CMTNS between the different CMT subgroups, and the US parameters (CSA and diameter) among the different CMT subgroups and controls, a Bonferroni-corrected Mann-Whitney U test was applied. The correlation between the US findings (CSA and diameter) and clinical parameters (age, height, weight, body mass index and CMTNS) or the electrophysiological parameters (DML, MCV, SCV, CMAP amplitude and SNAP amplitude) in controls and patients with CMT1A was tested with Pearson correlation coefficients. In all comparisons, a p value of less than 0.05 was considered significant. All statistical analyses were performed using STATA software (Stata Corp, Texas, USA).

RESULTS

Clinical data and CMTNS

On the basis of the genetic testing results, 20 patients were classified with *PMP 22* duplication-associated CMT (CMT1A), 3 with *MPZ*-associated CMT (2 CMT1B and 1 CMT2J), 4 with
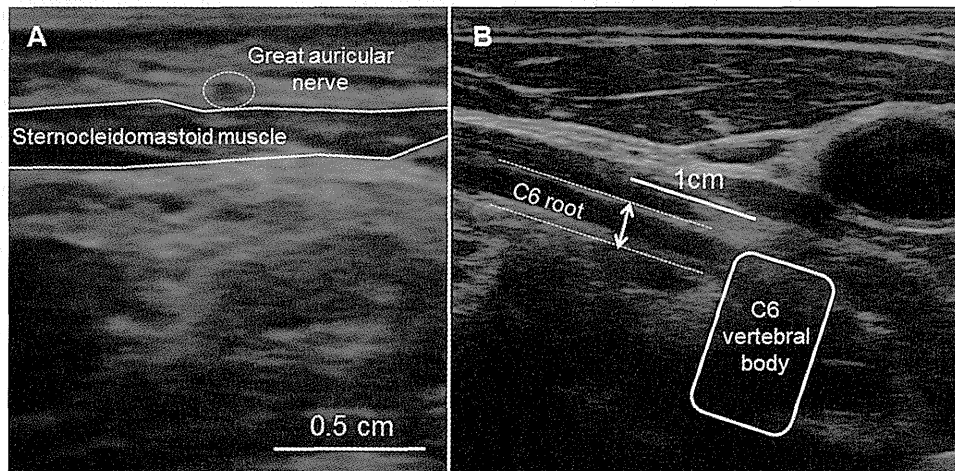
−39−

Figure 1 The ultrasound images of the great auricular nerve (A) and the measured site in the C6 nerve root (B). The dotted circle indicates the cross-sectional image of the great auricular nerve (A). The distances between the outer surfaces of the hyperechoic rims (between arrowheads) were measured as the nerve root diameter (B).

NEFL-associated CMT (2 CMT1F and 2 CMT2E), 1 with *EGR2*-associated CMT and 1 with *ARHGEF10*-associated CMT. The patient with CMT2J presented hearing loss and autonomic dysfunction such as Adie's pupils and dysuria, in addition to the distal dominant muscle weakness. All of the patients with *NEFL*-associated CMT showed distal dominant muscle weakness. The patient with *EGR2*-associated CMT was reported by us recently.[13] The patient with *ARHGEF10*-associated CMT presented muscle weakness in lower extremities with a slight decrease in vibratory sensation. Direct sequencing of the *ARHGEF10* gene in the patient with *ARHGEF10*-associated CMT revealed a heterozygous single nucleotide substitution, c.2435T>C, which might be a novel mutation. We could confirm the same mutation in the proband's brother with similar symptoms and electrophysiological findings, although gene analysis of other asymptomatic family members was not possible. No pathogenic mutation was identified in three patients with demyelinating type CMT and three with axonal type CMT.

Demographic data, the electrophysiological neuropathy type, CMTNS and gene mutation of each CMT subtype are shown in table 1. No significant difference in CMTNS was demonstrated among the CMT subtypes. In groups with *MPZ* or *NEFL* mutation, demyelinating and axonal types were mixed.

US findings

US findings in each CMT group and the control group are presented in table 2 and figure 2. The CSAs in patients with CMT1A were larger than those in controls irrespective of examination sites (figure 2). Although all mean CSAs and the C6 root diameter in patients with *MPZ* mutation tended to be larger than in controls, significant differences existed in the median nerve CSA at wrist and in the great auricular nerve CSA. There were no significant differences between all CSAs in patients with *NEFL* mutation and controls, whereas median nerve CSAs at three sites in patients with CMT1A were larger than in patients with *NEFL* mutation including the demyelinating type. In a patient with *EGR2* mutation, CSAs of proximal sites tended to be large, and the C6 root CSA in a patient with *EGR2* mutation was larger than the mean CSA value+2 SDs in controls. Although we could not identify the C6 root and great auricular nerve in a patient with *ARHGEF10* mutation, CSAs of the median nerve and sural nerve in the patient were slightly larger than the mean CSAs of controls.

Nerve conduction studies

Results of parameters of the NCS on the median and the sural nerves are listed in table 3. In patients with CMT1A, motor and

Table 1	Biometric data, electrophysiological neuropathy types, CMT Neuropathy Score and gene mutations					
	PMP22 duplication (n=20)	MPZ mutation (n=3)	EFL mutation (n=4)	EGR2 mutation (n=1)	ARHGEF10 mutation (n=1)	Controls (n=30)
Age, mean (range)	47.6 (21–78)	39.7 (10–69)	47.3 (27–68)	49	67	42.7 (24–84)
Gender (M/F)	10/10	2/1	2/2	0/1	1/0	19/11
Height (cm), mean (SD)	161.9 (10.0)	152.7 (16.1)	168.4 (5.1)	160.0 (NA)	173.5 (NA)	162.8 (11.5)
Weight (kg), mean (SD)	58.2 (11.1)	55.6 (17.5)	63.5 (22.2)	56.0 (NA)	76.0 (NA)	58.4 (10.8)
Body mass index, mean(SD)	22.1 (3.3)	23.4 (2.5)	22.3 (7.6)	23.8 (NA)	25.2 (NA)	21.9 (2.2)
Demyelinating type/axonal type	20/0	2/1	2/2	1/0	0/1	NA
CMT Neuropathy Score, mean (range)	14.0 (7–28)	12.0 (10–14)	15.5 (9–25)	7.0	7.0	NA
Gene mutations	PMP22 duplication	CMT1B: Tyr68Cys (n=2); CMT2J: Thr124Met	CMT1F: Pro8Leu (n=2) CMT2E: Glu396Lys; Tyr389Cys	Thr387Asn	Thr109Ile	NA

CMT, Charcot-Marie-Tooth disease; F, female; M, male; NA, not applicable.

−40−

Table 2 Ultrasound findings in patients with Charcot-Marie-Tooth disease and controls

	PMP22 duplication (n=20)		MPZ mutation (n=3)		NEFL mutation (n=4)		EGR2 mutation (n=1)		ARHGEF10 mutation (n=1)		Controls (n=30)	
	Mean (SD)	(n)	Mean (SD)	(n)	Mean (SD)	(n)	Mean (SD)	(n)	Mean (SD)	(n)	Mean (SD)	(n)
Cross sectional area (mm²)												
Median nerve (wrist)	23.5 (4.0)	(20)	21.0 (4.5)	(3)	12.0 (3.0)	(4)	20.5	(1)	22.8	(1)	14.1 (2.6)	(30)
Median nerve (forearm)	22.1 (9.2)	(20)	17.5 (8.9)	(3)	8.5 (3.1)	(4)	12.2	(1)	18.3	(1)	8.7 (1.3)	(30)
Median nerve (upper arm)	42.4 (11.8)	(20)	28.9 (12.3)	(3)	18.2 (4.4)	(4)	34.5	(1)	36.6	(1)	16.5 (2.7)	(30)
C6 root	29.8 (10.7)	(12)	17.0	(1)	17.1	(1)	42.2	(1)	NA	(0)	13.0 (3.1)	(22)
Great auricular nerve	3.9 (1.6)	(19)	5.2 (3.8)	(2)	2.0	(1)	3.5	(1)	NA	(0)	1.7 (0.6)	(25)
Sural nerve	11.0 (4.8)	(20)	7.5 (2.5)	(3)	6.0 (2.5)	(4)	6.7	(1)	14.3	(1)	5.8 (1.5)	(29)
Diameter (mm)												
C6 root	5.3 (1.1)	(13)	4.4	(1)	4.1	(1)	5.5	(1)	NA	(0)	3.6 (0.5)	(25)

NA, not applicable.

sensory conduction velocities reduced with decreased CMAP and SNAP amplitude. In patients with MPZ mutation, the patients with CMT1B had a very slow MCV, whereas the patient with CMT2J showed a nearly normal MCV. In patients with NEFL-mutations, the difference between CMT1F and 2E was similar to that between CMT1B and 2J. The patient with EGR2-associated CMT (CMT1D) showed a demyelinating pattern. The MCV and SCV were moderately slowed in the patient with ARHGEF10 mutation.

Correlation between US findings and clinical/electrophysiological parameters in patients with CMT1A

We analysed the correlation between US findings (nerve CSAs and C6 diameter) and clinical data (CMTNS, age, height, weight and body mass index)/electrophysiological parameters in patients with CMT1A. The CMTNS in patients with CMT1A was positively correlated with the CSA of the great auricular nerve and that of the median nerve at the upper arm (figure 3A, B). Moreover, an inverse association was noted between the C6 root CSAs and age
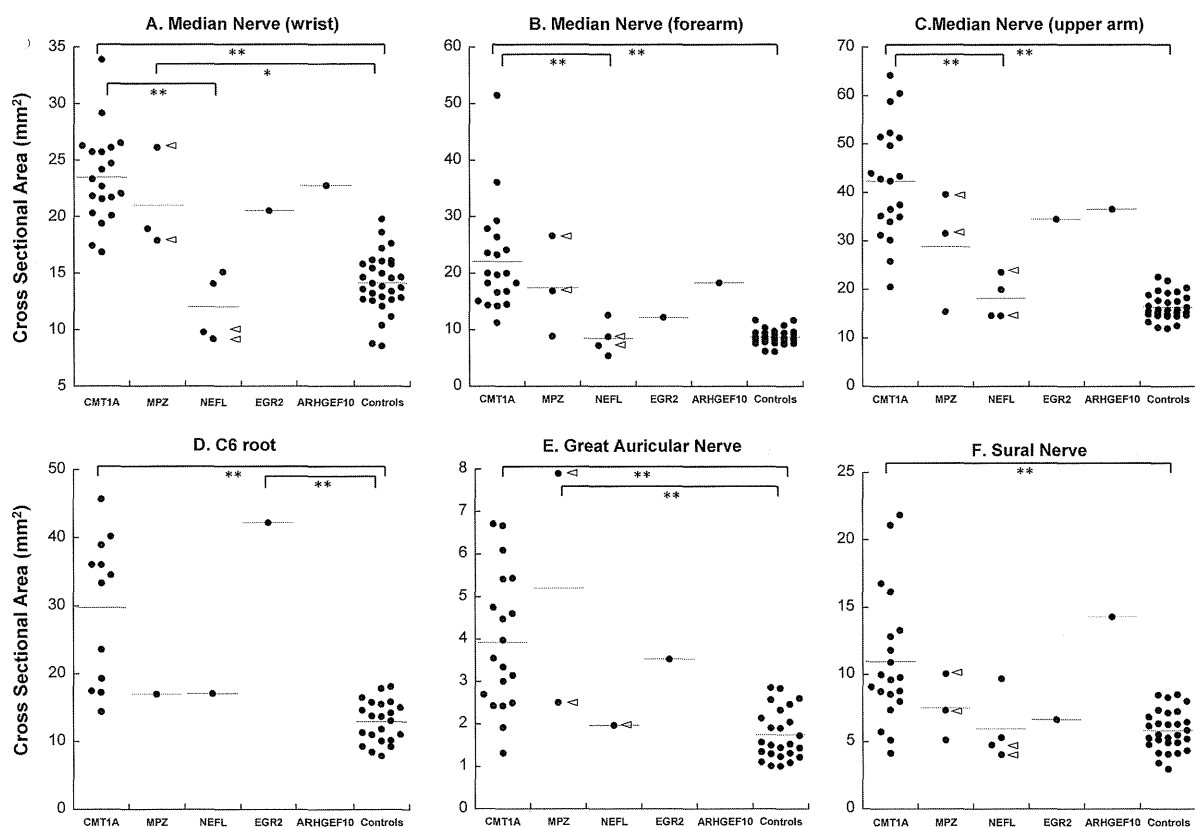
Figure 2 Ultrasound data on the median nerve, C6 root, great auricular nerve and sural nerve in patients with Charcot-Marie-Tooth disease (CMT) and controls. Horizontal bars indicate means. *p<0.05; **p<0.01. Arrowheads indicate demyelinating type in patients with MPZ-associated and NEFL-associated CMT. Cross-sectional areas of the C6 root and great auricular nerve in patients with ARHGEF10-associated CMT were not recorded because of technical difficulty in ultrasound examination.

Table 3 Nerve conduction study results

	Median nerve (motor)			Median nerve (sensory)		Sural nerve	
	DML (ms)	Amplitude (mV)	MCV (m/s)	Amplitude (µV)	SCV (m/s)	Amplitude (µV)	SCV (m/s)
PMP22 duplication (n=20)	10.2	3.8	21.8	1.3	20.9	0.6	22.9
MPZ mutation (n=3)							
CMT1B (n=2)	6.9	4	14.6	0.0	NA	0.0	NA
CMT2J (n=1)	3.7	11.3	46.4	9.7	49.4	6	51.9
NEFL mutation (n=4)							
CMT1F (n=2)	8.0	2.4	24.2	0.0	NA	0.0	NA
CMT2E (n=2)	5.7	9.8	50.4	6.8	43.5	1.3	54.9
EGR2 mutation (n=1)	6	4.7	23.2	2.1	26.8	NE	NA
ARHGEF10 mutation (n=1)	4.7	5.6	41.7	14.7	40.2	6.5	48.8

Data are given as means.
CMT, Charcot-Marie-Tooth disease; DML, distal motor latency; MCV, motor conduction velocity; NE, not evoked; NA, not applicable; SCV, sensory conduction velocity.

(figure 3C). Although statistically significant differences were not demonstrated, age tends to correlate inversely with CSAs of the median nerve at the fore arm, that at upper arm, the sural nerve and the great auricular nerve, whereas a positive relationship between age and CSAs of median nerve at the wrist was observed (p=0.23). All clinical data except for the CMTNS and age showed no correlation with CSAs and the C6 diameter.

In the analysis between US findings of the median nerve and electrophysiological parameters, there was a significant negative correlation between the CSA at the forearm and MCV of the median nerve (between the wrist and elbow; p<0.05; figure 4A). Likewise the CSA at the upper arm of the median nerve was negatively correlated with the MCV of the median nerve (between the wrist and elbow; p<0.01; figure 4B). No correlation was observed between the CSA and CMAP amplitude/SNAP amplitude of the median nerve. Analysis of the correlation between US and electrophysiological findings of the sural nerve was not performed because SNAPs were not evoked in 18 of the 20 patients with CMT1A.

DISCUSSION
In this study, we confirmed that patients with CMT1A showed a uniform enlargement of nerves, including the nerve root, based on US imaging. Although small in number, we showed increased CSA in median nerves in individuals with MPZ mutations (CMT1B and 2J), EGR2 mutations (CMT1D) and ARHGEF10 mutations. In patients with NEFL mutations (CMT1F and 2E), however, the CSAs in the examined nerves are comparable to those in normal controls. This is the first report regarding the US findings in patients with CMT2J, 1F, 2E, 1D and ARHGEF10-associated CMT. The limitation of this study included a small number of patients with rare mutations. Therefore, these findings should be confirmed in a larger cohort in the future. Furthermore, we revealed not only the presence of a correlation between the CSAs and electrophysiological parameters, but also a correlation between the CSAs and clinical parameters (CMTNS) in patients with CMT1A.

In agreement with previous reports, we found markedly increased CSAs in all nerves and nerve roots in patients with CMT1A.[6-9] [14] The ranges of CSAs in great auricular and sural nerves of patients with CMT1A and controls overlapped to some extent (figure 2). Measuring CSAs in the median nerve and nerve root may facilitate a clear distinction among CMT1A, NEFL-associated CMT and a healthy state. Pazzaglia et al[15] reported that the sural nerve CSA was not increased in the majority of patients with CMT1A (70%). In our study, however, the

sural nerve CSA in patients with CMT1A was significantly larger than that in controls. One of the factors influencing the difference between our results and the aforementioned study might be that CSAs were calculated by tracking the nerve circumference including the hyperechoic rim in that study. We measured CSAs by tracking the outline of the hyperechoic rim in consideration of the possibility that the nerve stroma including the epineurium proliferates in some subtypes of CMT. Robaglia-Schlupp et al[16] reported that PMP22 overexpression enhanced collagen synthesis by fibroblasts, and noted the possibility that structures other than Schwann cells were affected in CMT1A.

In this study, three patients with MPZ mutations were included. Two of them were diagnosed with CMT1B. The remaining patient was diagnosed with CMT2J. There have been no reports including US findings in patients with CMT2J. CSAs in all nerves of the patient with CMT2J were the smallest in the three patients with MPZ-associated CMT, and these, excluding the median nerve (wrist) of the patient with CMT2J, were nearly the same as the mean values of the control group. Median nerve CSAs of the other two patients with demyelinating-type MPZ-associated CMT (CMT1B) tended to be larger than in controls (figure 2). These findings are consistent with a previous study on CMT1B.[8]

This is the first report on nerve US findings including patients with NEFL-associated CMT. Four patients with NEFL-associated CMT were examined in this study, comprising two with CMT1F and two with CMT2E. Although two of the four patients had demyelinating-type CMT, they did not show the enlargement of peripheral nerves. The NEFL gene encodes the neurofilament light chain polypeptide (NEFL), which is one of the most abundant cytoskeletal components of neurons, and plays a pivotal role in the assembly and maintenance of the axonal cytoskeleton. Fabrizi et al[17] noted that the main pathological finding in patients with NEFL-associated CMT was axonopathy with marked structural alterations in the cytoskeleton and significant secondary demyelination. It appears that nerve conduction velocity slowing in NEFL-associated CMT is associated with mutations affecting the NEFL protein head domain.[18] From these findings, patients with demyelinating type CMT may not always present increased CSAs of nerves, although previous studies have reported that patients with other demyelinating type CMT generally showed increased CSAs of nerves.[9] [19]

The patient with EGR2-associated CMT in this study presented with a mild, demyelinating, adult-onset form.[13] The EGR2 gene encodes early growth response-2 protein (EGR2), which plays a role in peripheral nerve myelin development and maintenance, and

−42−

Neuromuscular

Figure 3 Scatterplot of the clinical parameters and ultrasound findings in patients with CMT1A. The CMTNS was positively correlated with the CSA of the great auricular nerve and that of the median nerve at the upper arm (A and B). An inverse correlation between the C6 root CSAs and age was observed (C). CMTNS, CMT neuropathy score; CSA, cross-sectional area; CMT, Charcot-Marie-Tooth disease.
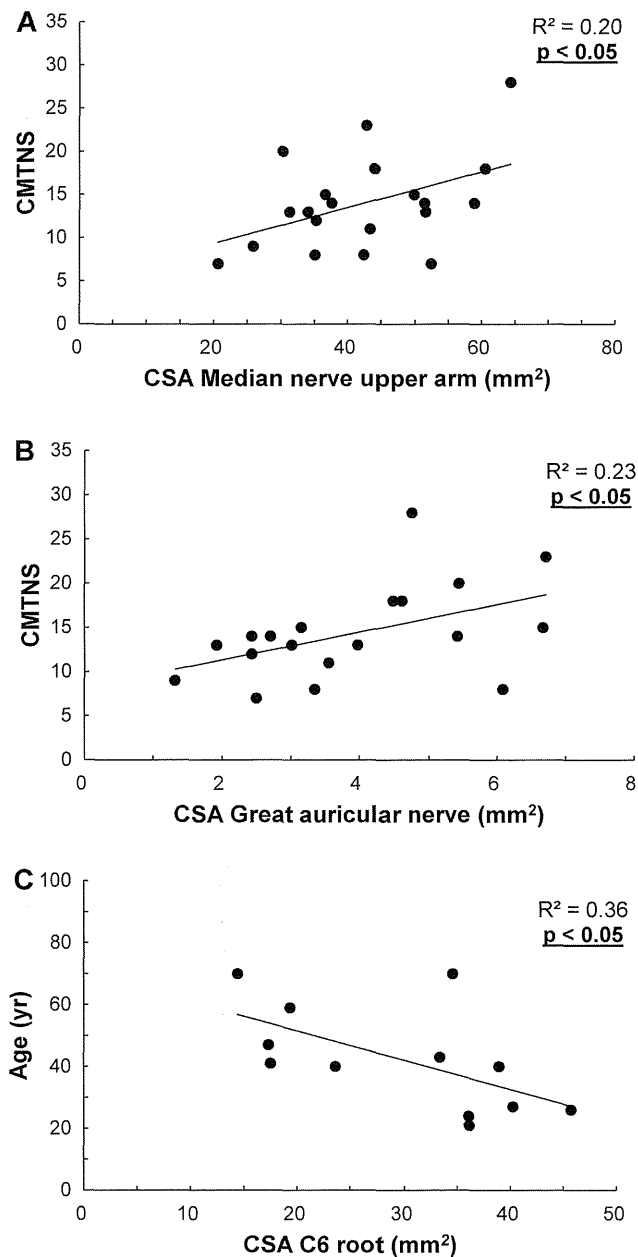

Figure 4 Scatterplot of the electrophysiological parameters and ultrasound findings in patients with CMT1A. A negative correlation between the CSA at the forearm and MCV of the median nerve (between the wrist and elbow) was found (A). Likewise the CSA at the upper arm of the median nerve was negatively correlated with the MCV of the median nerve (between the wrist and elbow) (B). CMT, Charcot-Marie-Tooth disease; CSA, cross-sectional area; MCV, motor conduction velocity.

activates the transcription of several myelin-associated genes, such as *PMP22* and *MPZ*. Although we could include only one patient with *EGR2*-associated CMT, CSAs in all nerves tended to be larger than in controls. We also included the patient with CMT who had a potent novel mutation in the *ARHGEF10* gene, as aforementioned. The phenotype of the patient was classified as the axonal type by neurophysiological testing, but the MCV was moderately slowed (median nerve MCV 41.7 m/s), as well as in previous studies.[20] [21] Verhoeven *et al* demonstrated the possibility that ARHGEF10 protein is associated with the developmental myelination of peripheral nerves using a mouse model. CSAs in all nerves were increased in the present patient, although CSAs of the C6 root and great auricular nerve were not recorded because of technical difficulties.
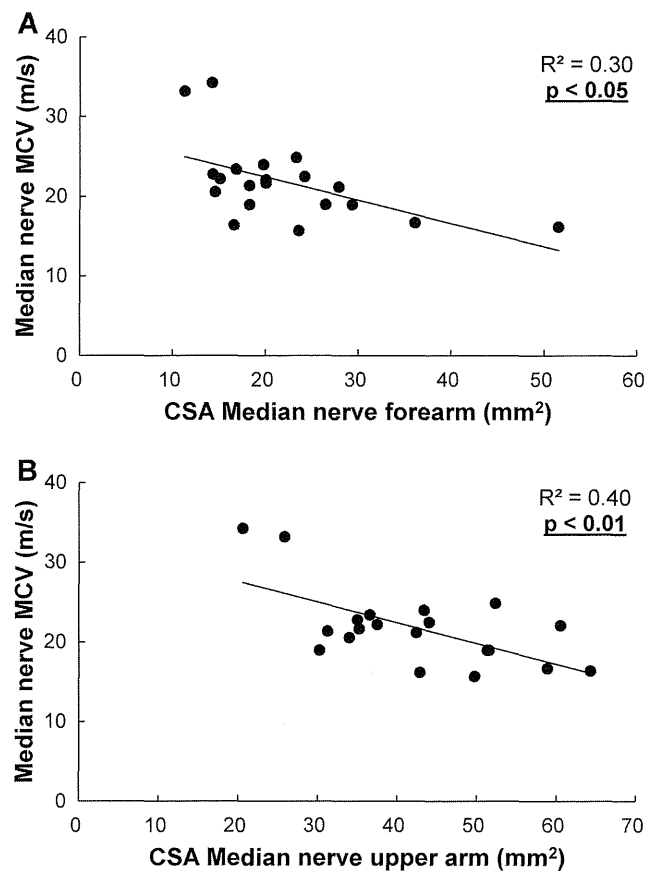
Regarding the US findings of the patients with CMT1A, Pazzaglia *et al*[15] demonstrated an inverse correlation between sural nerve CSAs and the age in patients with CMT1A. In this study, no such correlation was observed in patients with CMT1A. As aforementioned, the difference in the method of measuring CSAs could influence the results. Instead, a significant negative correlation between C6 root CSAs and the age was noted. However, there are some reports that the biometric data of patients with CMT showed no significant correlation with CSAs.[7] [9] Thus, the results of correlation analysis between CSAs and biometric data have varied among reports. The reason for this remains unclear, and so further studies involving larger series of cases are needed.

This study first showed the correlation between the disease severity (CMTNS) and CSAs in patients with CMT1A. Patients with a larger CSA in the median or great auricular nerve may show more marked impairment. It is extrapolated from these results that the degree of the disease severity might be determined by the extent of the pathological change, such as onion bulbs which are the results of repetitive demyelination–remyelination and the proliferation of the nerve stroma. On the other hand, it seems that the positive relationship between CMTNS and CSAs contradicts the inverse relationship between age and CSAs in this study (figure 3), because CMTNS generally increases with age in patients with CMT. Future studies will be

—43—

required to elucidate whether age or disease severity has more influence on the nerve enlargement in CMT1A. Along with the report by Pazzaglia et al,[15] the negative correlation between age and CSAs in most of the nerves might be specific to CMT1A, and indicates that decreased CSAs reflect axonal loss. Conversely, only CSA in median nerve at wrist correlated with age positively in patients with CMT1A of this study, although it was not statistically significant. CSA at wrist might be affected by factors except for CMT1A including carpal tunnel syndrome (CTS), etc. In patients with CTS, median nerve CSAs at wrist are generally increased.[22]

Several studies have reported on the relationships between US findings and NCS parameters in CMT and other neuropathies.[7] [9] [23-25] Consistent with a previous study by Schreiber et al, we identified a significant negative correlation between the CSAs of median nerve and the MCVs in the corresponding segment. The decreased MCVs in patients with CMT1A reflect the functional aspect for the histopathological alteration of myelination, progression of which might have paralleled the enlargement of nerves, that is, increased CSAs.

There are some limitations to our study. First, US examinations were performed by only one unblinded examiner. However, Cartwright et al[26] [27] reported that the diagnostic accuracy of neuromuscular US in unblinded studies was similar to that in blinded studies, and that intra-rater and inter-rater reliability of nerve and muscle US were sufficiently high. This argument may mitigate the unblinded design in this study to some extent; however, blinded assessment by multiple examiners is desirable in future studies on nerve US. Second, the small number of some CMT types is also a limitation of our study. Therefore, the findings of CSAs obtained from a single or a few patients should be carefully interpreted. Further study of a large population is needed, especially in MPZ-associated and NEFL-associated CMT in which demyelinating and axonal types are mixed. Third, the US feature of CMT1A has been already revealed by some studies.[5-7] [9] [14] However, describing the US finding of that was needed for shedding light on the extent of nerve enlargement in other rare CMT subtypes. In addition, nerve CSAs correlated with the clinical severity in CMT1A can provide a new insight into the evolving field of nerve US. Finally, our CSA measuring method including the hyperechoic rim is different from the method in most previous studies of nerve US with tracking inside the rim. Therefore, US findings in our study should be compared with other studies of nerve US with caution. However, our method might make it possible to assess the actual pathology of CMT because structures other than Schwann cells could proliferate in CMT1A.[16]

In conclusion, we have demonstrated US findings at diverse anatomical sites of patients with CMT subtypes. We confirmed the uniform enlargement of peripheral nerves in patients with CMT1A. We also found that patients with demyelinating-type CMT, such as CMT1F (NEFL-associated CMT), do not always exhibit nerve enlargement. Nerve US in addition to conventional NCS could facilitate targeted gene analysis in clinical situations, and may advance the understanding of peripheral nerve pathology in patients with CMT.

Contributions Y-iN was involved in design of the study, analysis of the data and drafting of the manuscript. KS was involved in design of the study, acquisition and interpretation of data and revision of the manuscript. YT was involved in interpretation of the data. IM was involved in acquisition and analysis of the data. YH, AH and HT were involved in acquisition and analysis of the data and drafting of the manuscript. MN was involved in design of the study and revision of the manuscript.

REFERENCES

1 Harding AE, Thomas PK. The clinical features of hereditary motor and sensory neuropathy types I and II. Brain 1980;103:259–80.
2 Shy ME, Siskind C, Swan ER, et al. CMT1X phenotypes represent loss of GJB1 gene function. Neurology 2007;68:849–55.
3 Murphy SM, Laura M, Fawcett K, et al. Charcot-Marie-Tooth disease: frequency of genetic subtypes and guidelines for genetic testing. J Neurol Neurosurg Psychiatry 2012;83:706–10.
4 Hattori N, Yamamoto M, Yoshihara T, et al. Demyelinating and axonal features of Charcot-Marie-Tooth disease with mutations of myelin-related proteins (PMP22, MPZ and Cx32): a clinicopathological study of 205 Japanese patients. Brain 2003;126:134–51.
5 Heinemeyer O, Reimers CD. Ultrasound of radial, ulnar, median, and sciatic nerves in healthy subjects and patients with hereditary motor and sensory neuropathies. Ultrasound Med Biol 1999;25:481–5.
6 Zaidman CM, Al-Lozi M, Pestronk A. Peripheral nerve size in normals and patients with polyneuropathy: an ultrasound study. Muscle Nerve 2009;40:960–6.
7 Martinoli C, Schenone A, Bianchi S, et al. Sonography of the median nerve in Charcot-Marie-Tooth disease. AJR Am J Roentgenol 2002;178:1553–6.
8 Cartwright MS, Brown ME, Eulitt P, et al. Diagnostic nerve ultrasound in Charcot-Marie-Tooth disease type 1B. Muscle Nerve 2009;40:98–102.
9 Schreiber S, Oldag A, Kornblum C, et al. Sonography of the median nerve in CMT1A, CMT2A, CMTX, and HNPP. Muscle Nerve 2013;47:385–95.
10 Zhao Z, Hashiguchi A, Hu J, et al. Alanyl-tRNA synthetase mutation in a family with dominant distal hereditary motor neuropathy. Neurology 2012;78:1644–9.
11 Matsuoka N, Kohriyama T, Ochi K, et al. Detection of cervical nerve root hypertrophy by ultrasonography in chronic inflammatory demyelinating polyradiculoneuropathy. J Neurol Sci 2004;219:15–21.
12 Shy ME, Blake J, Krajewski K, et al. Reliability and validity of the CMT neuropathy score as a measure of disability. Neurology 2005;64:1209–14.
13 Shiga K, Noto Y, Mizuta I, et al. A novel EGR2 mutation within a family with a mild demyelinating form of Charcot-Marie-Tooth disease. J Peripher Nerv Syst 2012;17:206–9.
14 Sugimoto T, Ochi K, Hosomi N, et al. Ultrasonographic nerve enlargement of the median and ulnar nerves and the cervical nerve roots in patients with demyelinating Charcot-Marie-Tooth disease: distinction from patients with chronic inflammatory demyelinating polyneuropathy. J Neurol 2013;260:2580–7.
15 Pazzaglia C, Minciotti I, Coraci D, et al. Ultrasound assessment of sural nerve in Charcot-Marie-Tooth 1A neuropathy. Clin Neurophysiol 2013;124:1695–9.
16 Robaglia-Schlupp A, Pizant J, Norreel JC, et al. PMP22 overexpression causes dysmyelination in mice. Brain 2002;125:2213–21.
17 Fabrizi GM, Cavallaro T, Angiari C, et al. Charcot-Marie-Tooth disease type 2E, a disorder of the cytoskeleton. Brain 2007;130:394–403.
18 Miltenberger-Miltenyi G, Janecke AR, Wanschitz JV, et al. Clinical and electrophysiological features in Charcot-Marie-Tooth disease with mutations in the NEFL gene. Arch Neurol 2007;64:966–70.
19 Zaidman CM, Harms MB, Pestronk A. Ultrasound of inherited vs. acquired demyelinating polyneuropathies. J Neurol 2013;260:3115–21.
20 De Jonghe P, Timmerman V, Nelis E, et al. A novel type of hereditary motor and sensory neuropathy characterized by a mild phenotype. Arch Neurol 1999;56:1283–8.
21 Verhoeven K, De Jonghe P, Van de Putte T, et al. Slowed conduction and thin myelination of peripheral nerves associated with mutant rho Guanine-nucleotide exchange factor 10. Am J Hum Genet 2003;73:926–32.
22 Nakamichi K, Tachibana S. Ultrasonographic measurement of median nerve cross-sectional area in idiopathic carpal tunnel syndrome: diagnostic accuracy. Muscle Nerve 2002;26:798–803.
23 Scheidl E, Bohm J, Simo M, et al. Ultrasonography of MADSAM neuropathy: focal nerve enlargements at sites of existing and resolved conduction blocks. Neuromuscul Disord 2012;22:627–31.
24 Watanabe T, Ito H, Sekine A, et al. Sonographic evaluation of the peripheral nerve in diabetic patients: the relationship between nerve conduction studies, echo intensity, and cross-sectional area. J Ultrasound Med 2010;29:697–708.
25 Tsukamoto H, Granata G, Coraci D, et al. Ultrasound and neurophysiological correlation in common fibular nerve conduction block at fibular head. Clin Neurophysiol 2014;125:1491–5.
26 Cartwright MS, Hobson-Webb LD, Boon AJ, et al. Evidence-based guideline: neuromuscular ultrasound for the diagnosis of carpal tunnel syndrome. Muscle Nerve 2012;46:287–93.
27 Cartwright MS, Demar S, Griffin LP, et al. Validity and reliability of nerve and muscle ultrasound. Muscle Nerve 2013;47:515–21.

−44−

JNNP

Nerve ultrasound depicts peripheral nerve enlargement in patients with genetically distinct Charcot-Marie-Tooth disease

Yu-ichi Noto, Kensuke Shiga, Yukiko Tsuji, et al.

Updated information and services can be found at:
http://jnnp.bmj.com/content/early/2014/08/04/jnnp-2014-308211.full.html

These include:

References	This article cites 27 articles, 6 of which can be accessed free at: http://jnnp.bmj.com/content/early/2014/08/04/jnnp-2014-308211.full.html#ref-list-1
P<P	Published online August 4, 2014 in advance of the print journal.
Email alerting service	Receive free email alerts when new articles cite this article. Sign up in the box at the top right corner of the online article.
Topic Collections	Articles on similar topics can be found in the following collections Neuromuscular disease (1162 articles) Peripheral nerve disease (581 articles) Radiology (1573 articles) Radiology (diagnostics) (1179 articles)

Advance online articles have been peer reviewed, accepted for publication, edited and typeset, but have not not yet appeared in the paper journal. Advance online articles are citable and establish publication priority; they are indexed by PubMed from initial publication. Citations to Advance online articles must include the digital object identifier (DOIs) and date of initial publication.

To request permissions go to:
http://group.bmj.com/group/rights-licensing/permissions

To order reprints go to:
http://journals.bmj.com/cgi/reprintform

To subscribe to BMJ go to:
http://group.bmj.com/subscribe/

Notes

Advance online articles have been peer reviewed, accepted for publication, edited and typeset, but have not not yet appeared in the paper journal. Advance online articles are citable and establish publication priority; they are indexed by PubMed from initial publication. Citations to Advance online articles must include the digital object identifier (DOIs) and date of initial publication.

To request permissions go to:
http://group.bmj.com/group/rights-licensing/permissions

To order reprints go to:
http://journals.bmj.com/cgi/reprintform

To subscribe to BMJ go to:
http://group.bmj.com/subscribe/

Neuromuscular

REVIEW

Ultrasound in the diagnosis of peripheral neuropathy: structure meets function in the neuromuscular clinic

Elena Gallardo,[1,2] Yu-ichi Noto,[3] Neil G Simon[4,5]

[1]Service of Radiology, University Hospital Marqués de Valdecilla; Instituto de Investigación Marqués de Valdecilla (IDIVAL), Santander, Spain
[2]University of Cantabria (UC); and Centro de Investigación Biomédica en Red de Enfermedades Neurodegenerativas (CIBERNED), Santander, Spain
[3]Department of Neurology, Graduate School of Medical Science, Kyoto Prefectural University of Medicine, Japan
[4]Prince of Wales Clinical School, University of New South Wales, Australia
[5]Central Clinical School, The University of Sydney, Australia

Correspondence to
Dr Neil G Simon, Prince of Wales Clinical School, University of New South Wales, Australia;
n.simon@unsw.edu.au

ABSTRACT

Peripheral nerve ultrasound (US) has emerged as a promising technique for the diagnosis of peripheral nerve disorders. While most experience with US has been reported in the context of nerve entrapment syndromes, the role of US in the diagnosis of peripheral neuropathy (PN) has recently been explored. Distinctive US findings have been reported in patients with hereditary, immune-mediated, infectious and axonal PN; US may add complementary information to neurophysiological studies in the diagnostic work-up of PN. This review describes the characteristic US findings in PN reported to date and a classification of abnormal nerve US patterns in PN is proposed. Closer scrutiny of nerve abnormalities beyond assessment of nerve calibre may allow for more accurate diagnostic classification of PN, as well as contribute to the understanding of the intersection of structure and function in PN.

INTRODUCTION

Peripheral neuropathy (PN) contributes significantly to the neurological burden of disease worldwide.[1 2] Prevalence of PN is increasing, particularly when associated with the growing population affected by diabetes,[3] and the rising incidence of drug-induced neuropathy associated with chemotherapy and antiretroviral drugs.[4 5]

Traditionally, the diagnostic work-up of PN involves delineating a pattern of clinical involvement through history and examination, with the diagnosis confirmed by neurophysiological studies. In some situations, the clinical features and associated comorbidities may be enough to diagnose PN without further investigations,[6] although grading of severity and monitoring of progression often includes neurophysiological assessment. However, the diagnosis of PN by clinical and neurophysiological grounds alone may be difficult, particularly in those patients with atypical or proximal demyelinating PN.[7] It may also be difficult to distinguish acquired from inherited demyelinating PN.[8] Hence, there is a need to develop novel strategies to aid in the diagnosis and monitoring of patients with PN, in particular the demyelinating forms.

The peripheral nervous system was unavailable to imaging modalities prior to the 1990s because of insufficient resolution and poor discrimination of nerves from surrounding soft tissues. However, recent technical developments have allowed imaging techniques, including MR neurography (MRN) and ultrasound (US), to play an important role in the diagnostic algorithm of peripheral nerve disorders. MRN currently provides an excellent depiction of three-dimensional nerve anatomy and pathology, and development of diffusion tensor imaging and tractography may provide further functional data.[9 10] US provides superior spatial resolution that has enabled detailed visualisation of even the smallest peripheral nerves. Evolution of high-frequency broadband transducers (up to 22 MHz), advances in image postprocessing and sensitive Doppler technology, that allows assessment of nerve vascularity without contrast administration, have improved the ability of US to detect anatomic details and subtle structural abnormalities in peripheral nerves. In addition, the acquisition of US is a real-time dynamic process and allows the examiner to explore the entire course of the nerve in a single sweep. Finally, US has the general advantages of being a painless, non-invasive and inexpensive technique. As such, US may be considered to be an optimal tool to look for structural nerve pathology, and hence serve as a complementary technique to clinical and neurophysiological diagnosis of patients with PN. This review will discuss the US features of PN, focusing on situations in which US studies may make a positive contribution to the diagnosis.

US FEATURES OF NORMAL PERIPHERAL NERVE

The US features of peripheral nerves correspond to macroscopic and microscopic anatomy.[11] Peripheral nerves are visualised on US as tubular structures with a characteristic fascicular appearance (figures 1 and 2). On longitudinal images, linear hypoechoic fascicles are seen, separated by bands of hyperechoic perineurial connective tissue. On axial images, the peripheral nerves demonstrate a 'honeycomb' appearance, with ovoid hypoechoic fascicles embedded in a hyperechoic background. The dense epineurial connective tissue surrounding the nerve is highly reflective of sound waves, which results in a hyperechoic rim that may provide a means of demarcating the nerve from surrounding structures.

There are some situations where the US appearance of normal nerves differs from a typical fascicular pattern. Nerves are more hypoechoic and demonstrate fewer or no fascicles in very proximal nerves, such as the brachial plexus and cervical nerve roots,[12] because of reduced volume of connective tissue and more tightly packed fascicles.[13] Echogenicity and fascicle number may also be reduced where they cross osteofibrous tunnels, such as the ulnar nerve in the cubital tunnel.[14] The size
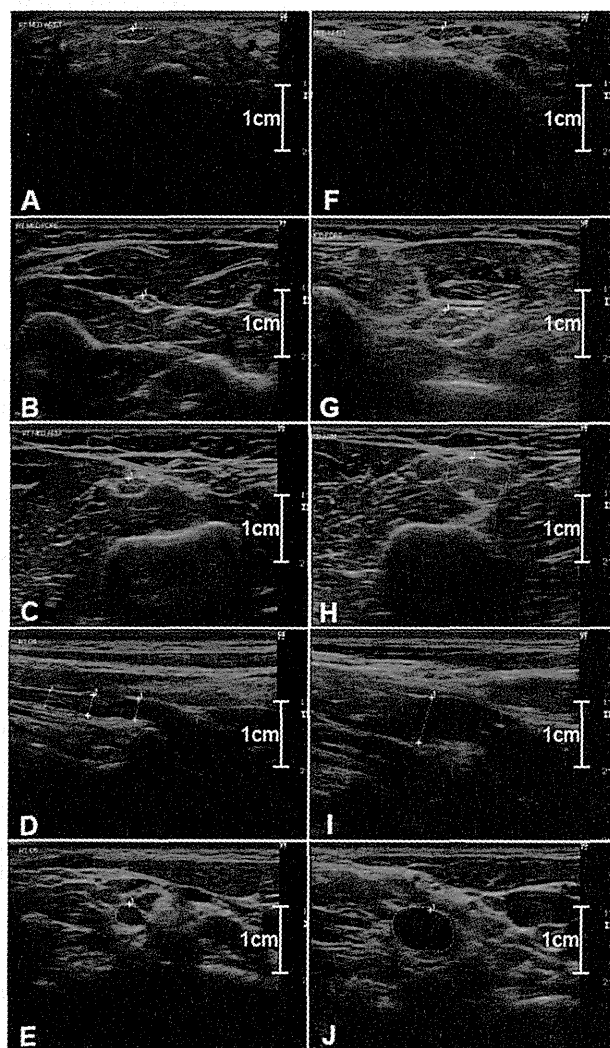
Figure 1 Ultrasound findings in Charcot-Marie-Tooth disease type 1A (CMT1A). Ultrasound images of the median nerve (wrist—A, mid-forearm—B, upper arm—C) and C6 nerve root (longitudinal—D, axial—E) in a healthy subject and a patient with CMT1A (wrist—F, mid-forearm—G, upper arm—H, C6 longitudinal—I, C6 axial—J) are depicted. Diffuse nerve enlargement was identified in the patient with CMT1A.

of peripheral nerves decreases slightly proximal to distal in the limb and it may be greater in entrapment sites in normal individuals.[14 15]

Commercially available US units are able to assess most peripheral nerves of the upper limbs, lower limbs and brachial plexus. However, very deep nerves such as the proximal sciatic nerve may be difficult to image, and the lumbar and sacral plexus cannot be visualised using US.

US FEATURES OF INJURED PERIPHERAL NERVE

US findings following peripheral nerve injury converge on a number of common features. These changes include alterations in nerve size, nerve echotexture, definition of the epineurial margins, fascicle diameter and vascularity. Much of the literature describing peripheral nerve changes following nerve injury is based on assessment of entrapment neuropathies.[16] In nerve compression, there may be focal nerve enlargement, loss of the internal fascicular appearance and decrease in nerve echogenicity.[17]

Nerve enlargement is most commonly quantified using cross-sectional area (CSA) traced within the hyperechoic epineurial

rim. CSA is a reliable measure with a good intraobserver and interobserver agreement and reproducibility;[18] therefore, it has been most frequently used to quantify changes in neuropathy and reference values have been established for the major limb nerves in several anatomic locations and for the brachial plexus.[15 19–21] It is worthwhile noting that some studies have demonstrated that nerve size may be influenced by age, gender, body mass index and height.[15 19] Temperature of the limb may also influence nerve calibre.[22] As such, it is recommended that comparison groups in studies of nerve US are matched for those subject characteristics and standardised environmental conditions are employed during the study.

Measuring the size of individual nerve fascicles may also contribute important pathophysiological information for the nerve injury and PN, although presently there is very little published data.[23] Fascicle size can differ between individuals, nerves and anatomic regions of an individual nerve, and hence a standardised approach would be required to systematically study this.

Peripheral nerve echogenicity may be quantified by measuring the mean grey scale value of the nerve image. Alternatively, thresholding techniques may be applied to determine the proportion of the nerve that is relatively hypoechoic.[14 24 25] Data obtained using each of these approaches is specific to the US system being used and cannot be compared with data from another site unless the values are calibrated using a universal phantom.

Nerve vascularity, as measured by Doppler, may also provide insights into the pathophysiology of peripheral nerve disease. In normal nerves there is no detectable blood flow.[26] Increased blood flow may be detected in compressive mononeuropathy and inflammatory PN,[16 27] possibly reflecting vascular proliferation precipitated by chronic trauma or inflammation (figure 3).

US FINDINGS IN PN

US is emerging as a valuable tool in the diagnosis of PN and it is in this field where it is anticipated that US will have a significant impact in rationalising the diagnostic pathway, potentially reducing the number of expensive investigations performed and focusing the use of expensive immunomodulatory therapies.[28] In this section, the US findings documented to date in hereditary, immune-mediated, infectious and axonal neuropathies will be discussed.

Hereditary neuropathies
Charcot-Marie-Tooth disease
Charcot-Marie-Tooth disease (CMT) is a clinically and genetically heterogeneous hereditary neuropathy characterised by distal muscle atrophy, weakness and sensory loss with reduced tendon reflexes. More than 60 different causative gene mutations have been described.[29] Nerve conduction studies still remain crucial both for the diagnosis and the classification of CMT (demyelinating type or axonal type), whereas US has emerged as a convenient technique to assess morphological changes of peripheral nerves in patients with CMT as a complement to the neurophysiological evaluation.

Nerve US findings of patients with CMT were first described in 1999 by Heinemeyer and Reimers [30] They examined nerve diameter, but not CSA, in patients with CMT. They concluded that nerve diameter and echogenicity did not differ significantly between patients with CMT and healthy subjects, and noted that the visualisation of nerves with the 7.5 MHz linear array probe was often difficult because of increased echogenicity of adjacent muscles in patients with CMT. The negative findings of this study may be explained by the limitations of resolution and

—48—